JOURNAL OF BAKU ENGINEERING UNIVERSITY - PHYSICS
2025. Volume 9, Number 2 *Pages 64-72*

UDC: 53.07
DOI: **https://doi.org/10.30546/09081.2025.002.1014**

INFLUENCE OF METALLIC HOST STRUCTURE ON MOLECULAR HYDROGEN EMBEDDED AND STABILITY UNDER ION IMPLANTATION

Alexandr DONKOV
International Intergovernmental Organization-Joint Institute for Nuclear Research, Dubna, Russian
Institute of Solid-State Physics, Bulgarian Academy of Sciences, Sofia, Bulgaria, aadonkov@theor.jinr.ru

Sekine ISAYEVA
Azerbaijan Technical University, Baku, Azerbaijan
sekinebagirli135@gmail.com

Aidos AKZHUNUSOV
L.N. Gumilyov Eurasian National University, Astana, Kazakhstan
aidos.akzhunussov89@gmail.com

Adiba MIRSAGATOVA
Institute of Nuclear Physics of the Uzbek Academy of Sciences, Tashkent, Uzbekistan
mirsagatova69@gmail.com

Alimardon RAKHIMOV
International Intergovernmental Organization-Joint Institute for Nuclear Research, Dubna, Russian
Institute of Nuclear Physics of the Uzbek Academy of Sciences, Tashkent, Uzbekistan, alimardon@jinr.ru

Bakhrom YARMATOV
Institute of Nuclear Physics of the Uzbek Academy of Sciences, Tashkent, Uzbekistan
yarmatov@inp.uz

Kiiril KREZHOV
Institute of Electronics, Bulgarian Academy of Sciences, Sofia, Bulgaria
kiril.krezhov@gmail.com

ARTICLE INFO

Article history:
Received: 2025-05-01
Received in revised form:2025-05-12
Accepted:2025-06-10
Available online:2025-12-21

Keywords:
High purity metal, ion implantation, annihilation, positron, hydrogen diffusion.

ABSTRACT

With this study we would like to confirm previously predicted computational results regarding the formation of molecular hydrogen during ion-metal interactions. The formation of defects in iron and titanium and their binding to hydrogen were analyzed using the positron lifetime method using calculations made with the MIKA software package. The observed decrease in the positron lifetime indicates a structural saturation with hydrogen, probably in its molecular form, and suggests the formation of $T(H)_2$ complexes in the induced cavities. These accumulations and additional hydride bonds act as barriers for hydrogen diffusion to the surface. For a perfect lattice in titanium in its hexagonal structure, a lifetime of 143 ps was calculated. For a vacancy with a few implanted atoms, we calculated a lifetime of 142 ps. For a perfect lattice for alpha iron, we obtained a value for the positron lifetime of 100 ps. An iron's vacancy with six implanted hydrogen atoms reports a lifetime of 101 ps.

1. INTRODUCTION

The challenges associated with the discovery and application of new energy sources remain one of the main driving forces in the development of human civilization [1]. The efficient utilization, storage, and transformation of energy resources have consistently formed the foundation of scientific and technological progress [2]. Advances in energy technologies have historically determined the pace of industrial growth, transportation development, and large-scale engineering achievements [3]. In this context, research focused on innovative energy conversion mechanisms is not only scientifically significant but also strategically essential for the future of humanity. In recent decades, the expansion of space exploration has led to new challenges related to energy extraction and the utilization of energy sources [4]. Renewed global interest in long-term space missions and potential colonization of planets near Earth has intensified the search for sustainable and efficient energy solutions. The possibility of long-term space travel critically depends on reliable propulsion systems and the continuous availability of fuel. Hydrogen, as a carrier for space propulsion, is a necessary product that provides a multitude of ancillary activities in space science [5]. To date, chemical combustion of hydrogen has been the main mechanism for propelling spacecraft. However, transporting sufficient quantities of hydrogen fuel for long-distance missions presents substantial logistical and technical challenges. This limitation naturally leads to a fundamental question: could hydrogen be generated directly in space using naturally available radiation environments, particularly the flux of high-energy protons emitted by the Sun? The concept of radiation-assisted hydrogen production and migration in metallic systems has been explored in previous studies. For example, Primakov et al. [6] investigated the acceleration of hydrogen diffusion in metals under gamma irradiation, particularly within environments simulating thermonuclear reactor conditions. In such systems, high-energy protons penetrate metallic structures, lose their kinetic energy within the bulk material, and subsequently participate in diffusion processes. The additional energy supplied by gamma radiation may enhance defect formation and atomic mobility, thereby facilitating hydrogen transport and potentially promoting recombination processes leading to molecular hydrogen formation. These observations indicate that ionizing radiation can play a dual role: first, by generating hydrogen in metal carriers by proton implantation, and second, by stimulating its migration and recombination from the formed metal hydride inside the lattice. Such a mechanism opens up the possibility of radiation-induced hydrogen accumulation in metallic structures exposed to cosmic rays. For a complete and practical cycle, however, attention must also be paid to the subsequent hydrogen management steps, including capture, stabilization, and controlled extraction (adsorption/desorption) of the formed molecular hydrogen. Understanding how hydrogen interacts with metal elements – its diffusion pathways, defect-assisted capture mechanisms, recombination behavior, and eventual release – is essential for assessing the feasibility of building a next-generation technology. Thus, the task that we set ourselves in this work is to propose a mechanism for selecting a suitable material in which after proton irradiation we can expect a product H_2. According to the work of Popov et al. [7] where iron and tungsten were used as host materials, the parameters that take into account the contribution of positron annihilation with valence and core electrons undergo an extremum and change their course. It is evident that at a certain point hydrogen forms bonds either with itself or in hydride form with the host metal. In the works of Pushilina et al. [8], Stepanova et al. [9], Laptev et al. [10], Bordulev et al. [11], Mikhailov et al. [12], Stepanova et al. [13], Mishin et al. [14] and Lider et al. [15] the phase transformation of titanium hydride and Zr-Nb base is considered, under different initial conditions. It is logical that when the valence electrons in the host material

are slightly inside the defects there will be less participation of ionized hydrogen in hydride form with the metal. It is for this reason that in the present work we compare the materials iron and titanium (which has a significantly lower valence than iron), in order to have a basis with which to continue our further work in this direction.

2. METHODS

MIKA: A software package [16] based on the TCDFT was used. The parameterized model in a localized electron gas is used to introduce the positron wave function. An improvement of Boronski and Nieminen [17] is introduced to approximate the volume correlation for electrons:

$$E_{xc}[n(r)] = \int n(r)\varepsilon_{xc}[n(r)]dr. \qquad (1)$$

$\varepsilon_{xc}[n(r)]$ is the single-particle exchange-correlation energy functional. The effective potential of Kohn and Sham is included in the work of Hohenberg, Kohn and Sham, where the DFT formalism accounting for the electron-positron interaction is considered. [18]. The momentum density is calculated separately for each electron state described by φ_j according to the equation:

$$\rho_j(p) = \pi r_0^2 cu(0) \text{ and } u = \frac{\lambda_j^{LDA}}{\lambda_j^{IPM}}. \qquad (2)$$

where IPM is Independent Particle Model [19]. The positron lifetime (τ) is the reciprocal of the annihilation rate (λ):

$$\lambda = \pi r_0^2 c \int dr n_{+e}(r) n_{-e}(r) \gamma = \pi r_0^2 c \sum_i \int dr. \qquad (3)$$

r_0 is the classical electron radius, c is the speed of light, γ is enhancement factor.

3. RESULTS AND DISCUSSION

Hydrogen implantation calculations in titanium and iron were performed by modeling a single vacancy cluster with an increasing number of hydrogen atoms (from one to six). The process simulates the formation of a hexagonal hydrogen structure (Fig. 1. a), b)), stabilized by internal pressure in the crystal lattice of both materials. The models used include a hexagonal lattice of 108 titanium atoms (space group $P6_3/mmc$) and a body-centered cubic (BCC) lattice of 250 iron atoms.

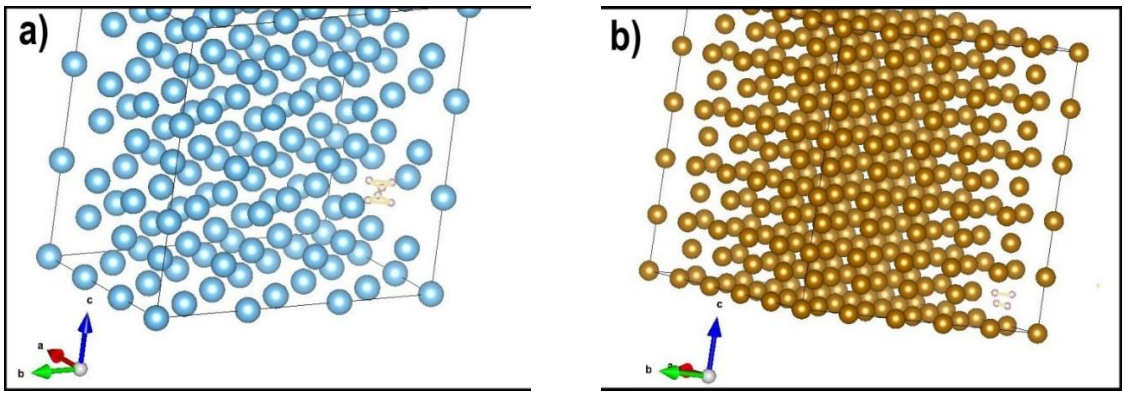

Figure 1. *Mono-vacancy and a hydrogen structure: (a) for titanium lattice with 6 implanted H atoms in defect; (b) for iron lattice with 4 implanted H atoms in defect.*

In the following figure (Fig. 2 a), b)) we present the dependence of the positron lifetime (τ), on the increasing number of hydrogen atoms, in a single-vacancy vacancy cluster – Fig. 2. A) – for the titanium crystal lattice, Fig. 2. B) – for the iron structure.

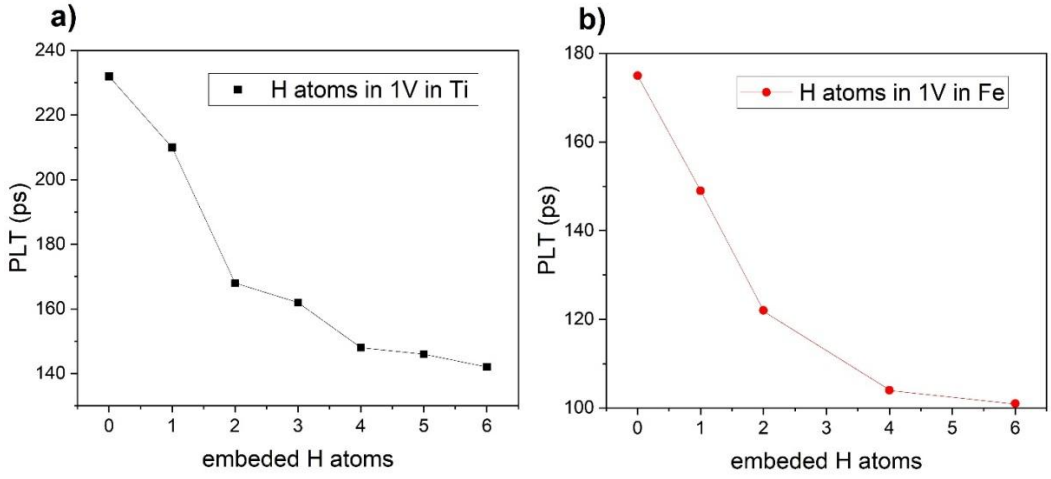

Figure 2. *τ as a function of the increasing number of hydrogen atoms in the vacancy cluster: a) for titanium, b) for iron.*

It is evident that in the significant difference between τ=100 ps, a perfect lattice for iron and τ=143 ps a perfect lattice for titanium, two factors play a major role - the arrangement of the atoms in space and the valence of the two elements. Regarding the arrangement of atoms in titanium, we have a close packing of the hexagonal type, while BCC is not a close packing, which means that although the arrangement is denser in titanium, the second factor - the valency - is essential and it is for this reason that the positron feels significantly freer in the titanium structure than in the iron one. The conclusion that we can make when implanting hydrogen atoms in the defect is similar - the electron density of a titanium lattice with a defect is significantly lower and respectively τ=142 ps with 6 embeded hydrogen atoms in a monovacancy, while for the same amount of embeded hydrogen atoms in an iron monovacancy τ=101 ps. The low electron density in titanium can be interpreted as a positive factor for transporting the hydrogen implanted in the defects, which at a certain point should bind in its molecular form. What has been said so far can be confirmed by the following figure (Fig. 3. a) - titanium, Fig. 3. b) - iron), where a ratio of the electron momentum density is determined in relation to the evolution of the increasing number of hydrogen atoms.

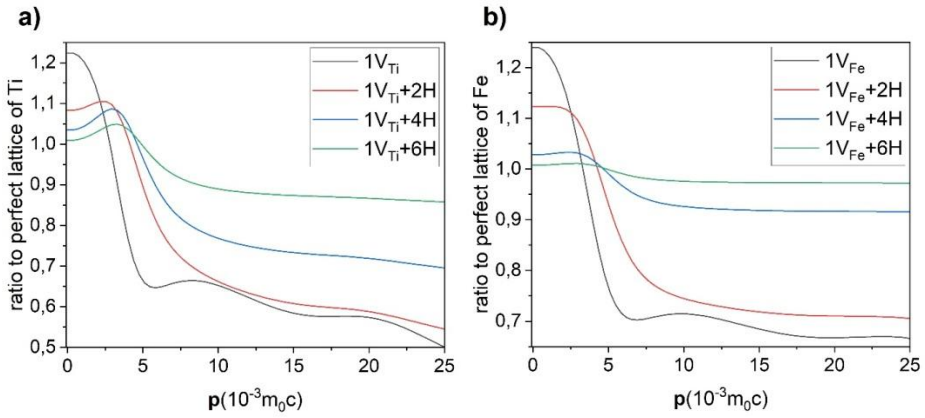

Figure 3. *Ratio of electron momentum density in mono-vacancy, mono-vacancy with 2, 4 and 6 hydrogen atoms, to a perfect lattice: a) for titanium, b) for iron.*

Directly from the last figure we can note the increased contribution of valence d-electrons to the annihilation in iron compared to titanium. It is seen how under the influence of hydrogen bonds with each subsequent accumulation of embedded hydrogen atoms, the valence sharply decreases, while at 6 hydrogens in the mono-vacancy the valence of the defect in iron is lower even than the valence of titanium under the same conditions. This in turn answers the question of what type a candidate for a host material should be, in the production of molecular hydrogen under radiation conditions, if it is a metal. On the one hand, this material should have a low valence and on the other hand, it should have high porosity in order to have suitable conditions for the removal of the hydrogen accumulated inside the defects. Studies have shown that the mechanism of formation of molecular hydrogen by proton implantation in porous materials is much slower. In Zr-based binary ceramic compounds, depending on the absorption dose of gamma quanta in their crystal structure, amorphization of oxide layers, mobilization of mono-vacancies, defect formation, recombination mechanism and functional groups decomposition, increase in crystallinity size due to structural rearrangement of oxygen ions, electron density, and different splitting of the energy levels of the material have been widely studied [20-21]. Gamma irradiation of ZrC and ZrB_2 induces the formation of Zr, B, and O vacancies through energy transfer processes associated with Compton scattering and secondary electron cascades, which generate atomic displacements in the crystal lattice [22]. Although γ-photons interact weakly with matter directly, the energetic electrons produced during irradiation can exceed the displacement threshold energy of lattice atoms, leading to the creation of point defects [23]. In ZrC, carbon vacancies typically form more readily due to their lower displacement energies compared to zirconium atoms, whereas in ZrB_2, boron vacancies are energetically favored over zirconium vacancies [24]. Oxygen-related vacancies may arise from impurity phases or surface oxidation layers, particularly under irradiation-enhanced diffusion conditions [25]. The formation and stabilization of vacancy clusters require cumulative energy on the order of several electron volts per defect, sufficient to overcome local binding energies and promote defect aggregation within the irradiated lattice [21], [23]. However, the mechanism of defect formation and vacancy formation in oxide and ceramic compounds by neutron irradiation is different. Neutron irradiation of boron trioxide (B_2O_3) leads to the formation of oxygen and boron vacancies through nuclear collisions and, in particular, through the $^{10}B(n,\alpha)\,^{7}Li$ reaction, which produces energetic recoil atoms capable of generating displacement cascades [26]. In titanium carbide (TiC), fast neutrons create both carbon and titanium vacancies, although carbon sublattice defects are typically more prevalent due to their lower displacement threshold energy, resulting in non-stoichiometry and possible vacancy clustering [27]. In cubic 3C-SiC, neutron bombardment induces silicon and carbon Frenkel pairs, antisite defects, and defect clusters, which may evolve into extended defects such as dislocation loops under higher doses [28]. In hexagonal boron nitride (h-BN), neutron interactions promote boron and nitrogen vacancy formation, with boron-rich defect configurations often stabilized by transmutation reactions and local lattice distortion [29]. The accumulation and interaction of these primary point defects under sustained neutron flux can lead to complex defect structures, including vacancy clusters and amorphization, depending on irradiation temperature and fluence [30-31]. Proton and helium irradiation of TiNbCN and TiSiCN coatings generates primary knock-on atoms that produce Frenkel pairs, with carbon and nitrogen vacancies forming preferentially due to their lower displacement threshold energies compared with Ti, Nb, or Si atoms. In TiSiCN, irradiation can additionally promote defect segregation at grain boundaries and within the amorphous Si-containing intergranular phase, influencing vacancy recombination and cluster stabilization [32]. Tungsten-based composites exposed to proton and helium beams exhibit vacancy accumulation

and helium–vacancy complex formation, which may evolve into nano-cavities or bubble-like features at elevated fluence and temperature [33-34]. The overall defect evolution in these materials depends strongly on ion energy, fluence, and microstructural features such as grain size and free volume, which govern defect migration, recombination, and clustering processes. Electron and heavy-ion irradiation of B_4C induces the formation of boron and carbon vacancies through displacement cascades, with heavy ions generating dense collision tracks that can locally amorphize the lattice and promote defect clustering [35]. In ZrB_2, energetic particles create zirconium and boron Frenkel pairs, and under high linear energy transfer conditions, vacancy aggregation may lead to dislocation loops or nanoscale defect complexes within the hexagonal lattice [36]. WC–6Co composites exposed to electron or heavy-ion beams exhibit vacancy formation both in the WC grains and in the cobalt binder phase, where radiation-enhanced diffusion can alter interfacial stability and promote defect segregation [37]. Heavy ions are particularly effective in producing localized thermal spikes, which facilitate the evolution of vacancy clusters, nano-cavities, or phase instability in these ceramics and cermets [38-39]. The extent of defect accumulation and structural modification depends on particle energy, fluence, and microstructural features such as grain size, binder distribution, and intrinsic free volume.

Examining in detail the works of Bordulev et al. [40] and Kudiiarov et al. [41], as well as following the logical thread from the introduction to this work of ours, we come to the conclusion that a magnesium base would be more suitable for our research. Continuing the logical sequence, we come to one of the main questions – "Could a better structural configuration be found at the nano level that would optimally determine the solution to the task we have set?". A similar dilemma is discussed in the work of Kudiiarov et al. [42], from 2023. From this, we can conclude that there is a collection of hydrogen in molecular form, which allows it to escape unhindered from the interior of the volume to the surface. At the same time, we should note that the participation of hydrogen in a chemical interaction with titanium is associated with the addition of additional energy [43], which practically facilitates our conclusions that chemical bonds are limited mainly to the molecular form of hydrogen. When we talk about adsorption of the produced hydrogen, we can mention several different methods. Alloys such as $TiFeH_2$ [44] and Mg_2NiH_4 [45] offer high capacity and reversible storage. On the other hand, the selective permeability of the polymer sites allows for controlled hydrogen release [46]. In this case, we recommend: Development of metal hydride-polymer hybrids adapted to extreme environments through material optimization and structural design [47]. Conducting experimental studies on radiation resistance and thermal cycling resistance [48]. Investigation of hybrid systems combining cryogenic adsorption with metal hydride-polymer technologies for synergistic benefits [49].

4. CONCLUSIONS

In titanium, chemical bonds in defects are mainly limited to the molecular form of hydrogen, while in iron there is an accumulation of hydride bonds with atoms close to the defect. Transport to the surface can be unhindered by the use of nanotubes made of low-valent material. In the adsorption of the formed molecular hydrogen, the development of a method for metal hydride-polymer hybrids adapted to extreme environments through material optimization and structural design, in combination with cryogenic adsorption, is recommended.

Acknowledgements

The authors wish to extend their sincere gratitude to Dr. E.P. Popov, Dr. S.F. Samadov, and Dr. of Sc. M.N. Mirzayev for their insightful recommendations and for providing essential support during the execution of this research.

REFERENCES

1. I.M. Peters, From fossil fuels to photovoltaics: Energy's role in human development and sustainability, EES Solar, Royal Society of Chemistry, 1 (2025) 712-723. DOI: 10.1039/D5EL00039D
2. Y. Zhao, M. Li, K. Wang, A. Sciacovelli, C. Qin, S. Lecompte, A.D. Thess. Thermo-mechanical energy storage technologies: Innovations, challenges and future directions. Front. Energy, 19(2) (2025) 115-116 DOI:10.1007/s11708-025-1007-3
3. P.W. Newton, P.W.G. Newman, S. Glackin, G. Thomson, Distributed green technologies for regenerating greyfields. In: Greening the Greyfields. Singapore. (2022) p71-87. https://doi.org/10.1007/978-981-16-6238-6_3
4. J. Zheng, L. Sun, X. Long, J. Wang, C. Li, Z. Mo, M. Du, T. Gao, E. Xia, B. Li, X. Xu, H. Xie, Electricity generation for lunar bases during construction and operation: Key technologies, challenges and development roadmap, Acta Astronautica, 236 (2025) 790-809. https://doi.org/10.1016/j.actaastro.2025.07.032
5. J. Bird, Z. Ao, A.C. Frey, N. Sell, A. Plummer, J.S.A. Dawe, O.J. Pountney, N. Sameh, S. Djurović, M.F. Iacchetti, A.C. Smith, C.M. Sangan, Cryogenic pumping of liquid hydrogen for aerospace propulsion, Progress in Aerospace Sciences, 160 (2026) 101155. https://doi.org/10.1016/j.paerosci.2025.101155
6. N.G. Primakov, Kazarnikov, V.V., Rudenko, V.A., & Gosudarstvennyj Nauchnyj Tsentr Rossijskoj Federatsii - Fiziko-Ehnergeticheskij Inst., Obninsk (Russian Federation). (1995).
7. E. Popov, T. Troev, L. Petrov, K. Berovski, S. Peneva, and B. Kolev, (2015).
8. N. Pushilina, A. Panin, M. Syrtanov, E. Kashkarov, V. Kudiiarov, O. Perevalova, R. Laptev, A. Lider, and A. Koptyug, Metals 8, 301 (2018).
9. E. Stepanova, N. Pushilina, M. Syrtanov, R. Laptev, and E. Kashkarov, International Journal of Hydrogen Energy 44, 29380 (2019).
10. R. Laptev, V. Kudiiarov, and N. Pushilina, Materials Today: Proceedings 19, 2084 (2019).
11. Y. S. Bordulev, R. S. Laptev, V. N. Kudiiarov, and A. M. Lider, AMR 880, 93 (2014).
12. A. A. Mikhaylov, T. S. Priamushko, M. N. Babikhina, V. N. Kudiiarov, R. Heller, R. S. Laptev, and A. M. Lider, Applied Surface Science 432, 85 (2018).
13. E. N. Stepanova, G. P. Grabovetskaya, I. P. Mishin, A. D. Teresov, and M. S. Syrtanov, in (Tomsk, Russia, 2018), p. 020295.
14. I. P. Mishin, G. P. Grabovetskaya, E. N. Stepanova, R. S. Laptev, and A. D. Teresov, Russ Phys J 62, 854 (2019).
15. A.M. Lider, V. V. Larionov, S. Xu, and R. S. Laptev, Russ J Nondestruct Test **55**, 928 (2019).
16. T. Torsti, M. Heiskanen, M.J. Puska, R.M. Nieminen, MIKA: multigrid-based program package for electronic structure calculations, Int. J. Quantum Chem. 91 (2) (2003) 171–176, https://doi.org/10.1002/qua.10397]
17. Boroński E, Nieminen RM (1986) Electron-positron density functional theory. Phys Rev B 34:3820–3831.
18. Sahni, V. (2004). The Hohenberg-Kohn Theorems and Kohn-Sham Density Functional Theory. In: Quantal Density Functional Theory. Springer, Berlin, Heidelberg. https://doi.org/10.1007/978-3-662-09624-6_4
19. M. Horbatsch, Independent particle model description of multiple ionization dynamics in fast ion-atom collisions, Phys. B Al. Mol. Opt. Phys. 25 (1592) 3797-3821.
20. M.N. Mirzayev, K.M. Hasanov, A.C. Parau et al., Effect of the C/N ratio modification on the corrosion behavior and performance of carbonitride coatings prepared by cathodic arc deposition, Journal of Materials Research and Technology, 27 (2023) p.1724-1738.

21. M.N. Mirzayev, M.Nasrabadi, N.Tiep et al., Determination of amorphization oxide layers, mobilization and functional groups on ZrC nanocrystals under high gamma irradiation, Vacuum, Volume 238, 2025, 114215, https://doi.org/10.1016/j.vacuum.2025.114215.
22. S.F. Samadov, O.A. Samedov, D.M. Mirzayeva et al., Effect of gamma irradiation and thermal annealing on defect formation in ZrB2 nanocrystals, Physica B: Condensed Matter, Volume 717, 2025, 417807, https://doi.org/10.1016/j.physb.2025.417807.
23. M.N. Mirzayev, Oxidation kinetics of boron carbide ceramic under high gamma irradiation dose in the high temperature, Ceramics International, 46 (3), (2020) p.2816-2822.
24. M.N. Mirzayev, A.S. Abiyev, O.A. Samedov ety al., Structural evolution of zirconium diboride under gamma irradiation and thermal annealing. Journal of Alloys and Compounds. 1005, 2024, 175970. https://doi.org/10.1016/j.jallcom.2024.175970
25. S.F. Samadov, A.G. Asadov, A.S. Abiyev et al., Evaluation of nanocrystalline ZrC under gamma irradiation and high pressure. Physica B: Condensed Matter. Volume 688, 2024, 416154. https://doi.org/10.1016/j.physb.2024.416154
26. S.F. Samadov, N.V.M. Trung, A.A. Donkov et al., Investigating the impact of gamma irradiation and temperature on vacancy formation and recombination in ZrB_2 ceramics using positron annihilation spectroscopy. Journal of Nuclear Materials. 599, 2024, 155242. https://doi.org/10.1016/j.jnucmat.2024.155
27. M.N. Mirzayev, Simultaneous measurements of heat flow rate and thermal properties of nano boron trioxide under neutron irradiation at the low and high temperature, Vacuum, 173 (2020) p.109162.
28. E. Popov, L. Slavov, E. Demir et al., Microstructural evolution of TiC nano powders under fast neutron irradiation: A multi-technique analysis, Vacuum, 215 (2023) p.112338.
29. M.N. Mirzayev, High-flux neutron irradiation of boron trioxide analyzed with Raman and FTIR spectroscopy, International Journal of Modern Physics B, 34 (18) (2020) p.2050160.
30. M.N. Mirzayev, B.A. Abdurakhimov, E. Demir et., Investigation of the formation of defects under fast neutrons and gamma irradiation in 3C-SiC nano powder, Physica B: Condensed Matter., 611 (2021) p. 412842.
31. M.N. Mirzayev, Heat transfer of hexagonal boron nitride (h-BN) compound up to 1 MeV neutron energy: Kinetics of the release of wigner energy, Radiation Physics and Chemistry, 180 (2021) p.109244.
32. M.N. Mirzayev, L.Slavov, A.Donkov et al., Effects of neutron irradiation at different fluencies on nanosized anatase titanium dioxide, Radiation Physics and Chemistry, 194 (2022) p.109988.
33. A. Vladescu, M.N. Mirzayev, A.S. Abiyev et al., Effect of Si and Nb additions on carbonitride coatings under proton irradiation: A comprehensive analysis of structural, mechanical, corrosion, and neutron activation properties, Nuclear Materials and Energy, 35 (2023) p.101457.
34. E. Demir, M.N. Mirzayev, E.P. Popov et al., Effects of high-energetic 3He+ ion irradiation on tungsten-based composites, Vacuum, 184 (2021) 109934.
35. D. Neov, L. Slavov, A.A. Donkov et al., Structural study of W2B obtained via mechanical alloying of W, B4C, TiC and graphite before and after He ions irradiation, Nuclear Materials and Energy, 31 (2022) p.101201
36. M.N. Mirzayev, Study thermodynamic assessment of the B-C and B-Si binary systems with swift heavy ions and high intense electron beam irradiation at the low temperature, Modern Physics Letters B, 34(34) (2020) p.2050395.
37. M.N. Mirzayev, E. Popov, E. Demir et al., Thermophysical behavior of boron nitride and boron trioxide ceramics compounds with high energy electron fluence and swift heavy ion irradiated, Journal of Alloys and Compounds, 834 (2020) p.155119.
38. S.F. Samadov, A.S. Abiyev, A.G. Asadov et al., Investigating the crystal structure of ZrB_2 under varied conditions of temperature, pressure, and swift heavy ion irradiation, Ceramics International, 2023, https://doi.org/10.1016/j.ceramint.2023.11.125
39. E. Demir, E.Popov, M. Mirzayev et al., Effects of swift heavy ions at different fluencies on WC-6Co hard metal alloy, International Journal of Refractory Metals and Hard Materials, 106 (2022) p.105865.
40. I. Bordulev, R. Laptev, V. Kudiiarov, R. Elman, A. Popov, D. Kabanov, I. Ushakov, and A. Lider, Materials 15, 1823 (2022).

41. V.N. Kudiiarov, A. Kenzhiyev, R. R. Elman, N. Kurdyumov, I. A. Ushakov, A. V. Tereshchenko, R.S. Laptev, M. A. Kruglyakov, and P. I. Khomidzoda, Metals 15, 72 (2025).
42. V. Kudiiarov, R. Elman, N. Kurdyumov, and R. Laptev, Journal of Alloys and Compounds 953, 170138 (2023).
43. A. Lider, V. Kudiiarov, E. Kashkarov, M. Syrtanov, T. Murashkina, A. Lomygin, I. Sakvin, D. Karpov, and A. Ivanov, Metals 10, 880 (2020).
44. E.M. Dematteis, N. Berti, F. Cuevas, M. Latroche, and M. Baricco, Mater. Adv. 2, 2524 (2021).
45. A. Alaoui-Belghiti, A. Assila, I. Belkoufa, M. Rkhis, S. Laasri, M. Tlemçani, E. Hlil, and A. Hajjaji, International Journal of Hydrogen Energy 92, 1069 (2024).
46. M. Tian, S. Rochat, K. Polak-Kraśna, L. T. Holyfield, A. D. Burrows, C. R. Bowen, and T. J. Mays, Adsorption 25, 889 (2019).
47. J. C. Crivello, B. Dam, R. V. Denys, M. Dornheim, D. M. Grant, J. Huot, T. R. Jensen, P. De Jongh, M. Latroche, C. Milanese, D. Milčius, G. S. Walker, C. J. Webb, C. Zlotea, and V. A. Yartys, Appl. Phys. A 122, 97 (2016).
48. V. Bérubé, G. Radtke, M. Dresselhaus, and G. Chen, Int. J. Energy Res. 31, 637 (2007).
49. K. J. Jeon, H.R. Moon, A.M. Ruminski, B. Jiang, C. Kisielowski, R. Bardhan, J. J. Urban, Nature Mater 10, 286 (2011).